



Geophysical Research Letters°

RESEARCH LETTER

10.1029/2021GL096315

Key Points:

- Delta shape, especially shoreline curvature, constrains post-avulsion river mouth locations on waveinfluenced deltas
- Greater wave-climate asymmetry increases (decreases) shoreline diffusivity on the updrift (downdrift) flank, favoring downdrift avulsions
- Under some wave climates, reduced diffusivity on the downdrift flank leads to convex curvature that inhibits downdrift avulsions

Supporting Information:

Supporting Information may be found in the online version of this article.

Correspondence to:

N. Hu, ningjie.hu@duke.edu

Citation:

Hu, N., Murray, A. B., Ratliff, K. M., Little, Z., & Hutton, E. W. H. (2022). Wave-climate asymmetry influence on delta evolution and river dynamics. *Geophysical Research Letters*, 49, e2021GL096315. https://doi. org/10.1029/2021GL096315

Received 15 OCT 2021 Accepted 5 APR 2022

Author Contributions:

Conceptualization: Ningjie Hu, A. Brad Murray, Katherine M. Ratliff Data curation: Ningjie Hu Formal analysis: Katherine M. Ratliff, Zachary Little

Funding acquisition: A. Brad Murray Investigation: Ningjie Hu, A. Brad Murray, Katherine M. Ratliff Methodology: Ningjie Hu, A. Brad Murray, Katherine M. Ratliff Project Administration: Ningjie Hu, A. Brad Murray

Resources: Ningjie Hu, A. Brad Murray, Katherine M. Ratliff, Eric W. H. Hutton Software: Ningjie Hu, Katherine M. Ratliff

Supervision: A. Brad Murray **Validation:** Ningjie Hu, Katherine M. Ratliff

Visualization: Ningjie Hu

© 2022. American Geophysical Union. All Rights Reserved.

Wave-Climate Asymmetry Influence on Delta Evolution and River Dynamics

Ningjie Hu¹, A. Brad Murray¹, Katherine M. Ratliff¹, Zachary Little², and Eric W. H. Hutton³

¹Division of Earth and Climate Sciences, Nicholas School of the Environment, Duke University, Durham, NC, USA, ²Department of Biological and Agricultural Engineering, North Carolina State University, Raleigh, NC, USA, ³Community Surface Dynamics Modeling System, University of Colorado Boulder, Boulder, CO, USA

Abstract On wave-influenced river deltas, wave-driven sediment redistribution affects river progradation, and therefore avulsions, while avulsions change where sediment is delivered to the coastline, affecting coastline shape. Coastline shape, in turn, affects sediment redistribution rates and patterns. Here we use a numerical model to investigate how the asymmetry of wave climates affects delta avulsion behaviors, which are coupled with delta shape evolution. Increasing wave-climate asymmetry tends to reduce (increase) the curvature of updrift (downdrift) delta flanks, by increasing (decreasing) local shoreline diffusivity. In our model experiments, reduced shoreline curvature restricts the possible updrift post-avulsion river mouth locations, while increased curvature expands the possible downdrift locations, favoring "downdrift avulsions." However, under some wave climates, local diffusivity on the downdrift flank can become negative, leading to convexity and shoreline accretion, inhibiting downdrift avulsions. Increasing wave heights and decreasing superelevation threshold for avulsions both tend to reduce delta morphologic asymmetry, and therefore avulsion tendency.

Plain Language Summary On wave-influenced river deltas, wave-driven sand redistribution along the coastline affects the abandonment of previous river channels (i.e., river avulsion), and where new channels can form. The new river mouth location determines where sand is delivered to the coastline, affecting coastline shape, which in turn affects wave-driven sand redistribution. Here we use a numerical model to investigate how delta shape and river mouth locations are influenced by which directions waves tend to approach the coastline from. When waves approach the coastline from a dominant direction more often (i.e., increased wave-climate asymmetry), the wave-driven shoreline smoothing effect on the updrift delta flank is locally increased, creating a straighter shoreline. In contrast, the effectiveness of shoreline smoothing tends to decrease on the downdrift flank. Under such conditions, the river tends to avulse to the downdrift flank. However, under certain conditions, the wave smoothing effect on the downdrift flank can become negative (shoreline shapes become exaggerated), and shorelines tend to grow seaward, which inhibits downdrift avulsions. Additionally, we found that the maximum potential local wave smoothing effect, which could be realized for a particular local shoreline orientation, increases with wave-climate asymmetry—an insight with implications for coastline evolution beyond the scope of deltas.

1. Introduction

River deltas are dynamic depositional landforms formed by the coordination of fluvial and marine processes (Wright & Coleman, 1973). More than half a billion people live on or near deltas because these regions are biodiverse, with highly productive and fertile lands (Syvitski et al., 2009). Changes in the shape of deltas can affect humans directly. Therefore, informed decision-making about coastal and river management requires the understanding of natural processes that control delta formation and evolution. Although the influence of diverse natural processes (e.g., waves, tides, rivers) on delta morphology has long been discussed (A. D. Ashton & Giosan, 2011; Chatanantavet et al., 2012; Galloway, 1975; Nienhuis et al., 2015, 2018; Orton & Reading, 1993), the feedbacks among multiple natural processes, such as wave and river processes, and their impacts on delta morphology, remain to be better understood.

River delta morphology reflects the balance between sediment delivery by rivers to the coast and sediment reworking through waves and tides (Galloway, 1975). Because of anthropogenic reductions of river sediment input and increased rates of sea level rise, many river deltas have shifted toward wave or tide dominance (Nienhuis et al., 2020). The location and size of delta lobes are controlled by river avulsion dynamics. Avulsions tend

HU ET AL. 1 of 10



Writing – original draft: Ningjie Hu Writing – review & editing: Ningjie Hu, A. Brad Murray, Katherine M. Ratliff, Zachary Little, Eric W. H. Hutton to occur where the riverbed becomes sufficiently superelevated relative to its surrounding floodplain (Mohrig et al., 2000). In the context of deltas, avulsions typically occur at a distance from the river mouth that scales with the backwater zone (Chadwick et al., 2019; Chatanantavet et al., 2012; Ganti et al., 2016; Jerolmack, 2009; Ratliff et al., 2021). The backwater length (L_B) is approximated by the ratio of a characteristic flow depth (bankfull channel depth here) and riverbed slope (Paola, 2000).

On wave-influenced deltas, the deposition of sediment at the river mouth drives the shoreline to prograde seaward, while waves tend to distribute sediment along the shoreline. For a given wave climate, the rate of alongshore sediment flux depends on the local shoreline orientation (A. Ashton et al., 2001; A. D. Ashton & Murray, 2006a). Where a coastline is curved, the alongshore variation in shoreline orientation tends to create a gradient in alongshore sediment flux (Komar, 1973). The alongshore gradient in sediment flux, in turn, leads to shoreline erosion or accretion (A. Ashton et al., 2001; A. D. Ashton & Murray, 2006a). Shoreline curvature is the second derivative of cross-shore shoreline position, with respect to the alongshore direction. Under most wave climates, the flux of sediment alongshore tends to converge when the shoreline has a concave-seaward curvature, causing accretion, and diverge with a convex-seaward shoreline curvature, causing erosion (A. D. Ashton & Murray, 2006a; Dean & Yoo, 1992; Lauzon et al., 2019). Under such wave climates, alongshore transport tends to smooth the shoreline on the regional scale. When the range of shoreline orientations is small, this process can be treated as diffusion of the shoreline position, with positive diffusivity corresponding to coastline smoothing and negative diffusivity corresponding to coastline roughening (A. Ashton et al., 2001; A. D. Ashton & Murray, 2006a; Falqués & Calvete, 2005). The wave climate influences how rapidly a coastline tends to be smoothed—or equivalently, the effective long-term shoreline "diffusivity" (A. D. Ashton & Murray, 2006b). The same set of waves far offshore affect shorelines with different orientations differently, so that local shoreline diffusivity can vary from one place to another along a coast (A. D. Ashton & Murray, 2006b).

Recent numerical modeling works have provided basic insights on how waves influence delta morphology, including exploring the process of wave-driven alongshore sediment transport that redistributes fluvial sediment (A. D. Ashton et al., 2013), the control of wave directions on delta morphologies and morphodynamics (A. D. Ashton & Giosan, 2011), and the effect of asymmetric wave climates on plan-view deltas morphologies (A. D. Ashton & Giosan, 2011; Nienhuis et al., 2015). These works involved a channel position that is fixed in the alongshore direction. Nienhuis et al. (2016) examined the feedbacks between waves and river-mouth migration. Gao et al. (2020) continued the work and explored the impact of wave climate asymmetry on deltaic river-mouth morphodynamics. Ratliff et al. (2018) coupled wave-driven delta morphodynamics and river avulsion dynamics under a symmetric wave climate. However, how river avulsion dynamics and delta morphodynamics depend on the wave asymmetry has not previously been addressed.

Asymmetric wave climates drive net alongshore sediment transport toward the "downdrift" direction. Here, we present numerical modeling results demonstrating that wave-climate asymmetry can strongly influence river avulsion dynamics as well as plan-view river delta morphology. The delta model couples the River Avulsion and Floodplain Evolution Model (RAFEM, Ratliff et al., 2018) and the Coastline Evolution Model (CEM; A. Ashton et al., 2001; A. D. Ashton & Murray, 2006a) through the Community Surface Dynamics Modeling System Basic Model Interface (Peckham et al., 2013). The coupled delta model can be used to explore how ocean and river conditions influence delta evolution over large space and time scales (e.g., multiple river avulsion and delta lobe-building events), and how both delta planform shapes and longitudinal river and floodplain profiles evolve.

2. Methods

2.1. Model Summary

In RAFEM, fixed square cells contain information about riverbed, floodplain, or seafloor elevations (Ratliff et al., 2018). The initial river course is determined using a steepest-descent algorithm developed by Jerolmack and Paola (2007). Any cells the river course passes through are designated as river cells. Cell widths are an order of magnitude larger than the characteristic river width. A river cell includes information of riverbed elevation and levee height (assumed to be one bankfull channel depth above the riverbed). The morphodynamic evolution of the longitudinal river profile is modeled as a linear diffusive process (Jerolmack & Paola, 2007). The river diffusion coefficient represents the combined effect of long-term average water discharge and sediment characteristics (Ratliff et al., 2018). The bed elevation at the river mouth is one channel depth below sea level (Ratliff

HU ET AL. 2 of 10



et al., 2018). As the riverbed aggrades, driven by either progradation or sea-level rise, some portion of the river channel will become super-elevated relative to its surrounding floodplain. The normalized superelevation ratio (SER) is the difference between the levee crest elevation and the elevation of the adjacent floodplain, normalized by bankfull channel depth. A potential avulsion is triggered where the riverbed elevation meets or exceeds the critical superelevation ratio. Studies of river bifurcations show that a shorter path to the base level, with a steeper channel bed gradient and increased sediment transport capacity, tends to become the dominant flow path (Pittaluga et al., 2003; Slingerland & Smith, 2004). In the model, from a potential avulsion location, a new steepest-descent path to the sea is determined. If the new path is shorter than the prior path, then the river course will relocate to the new path, and the avulsion is successful. The old channel is filled to the average elevation of the surrounding floodplain cells (Ratliff et al., 2018). If the new path to the sea is longer than the previous river course, a crevasse splay will be deposited in the first cell where the avulsion is failed and its surrounding adjacent cells at a rate equaling to the in-channel aggradation rate just upstream of the splay, and avulsion does not occur. We tested critical SER values of 0.5 and 1 for model experiments based on the range suggested by field measurements (Hajek & Wolinsky, 2012). We nondimensionalized time and length with channel-filling time scale (T_{cp}) the amount of time it would take to fill one bankfull channel depth, if the river sediment flux was completely retained in the backwater zone, Text S1 in Supporting Information S1) and back-water length (L_B, the ratio of channel depth and riverbed slope), respectively. Wave height (WH) is nondimensionalized by the river channel depth. The processes described in the model are generic and potentially applicable to a range of delta types and sizes. For example, T_{cf} and L_B can range from decades and 1 km, respectively, for a small river (such as the model parameters we used in Table S1 in Supporting Information S1) to the millennial scale and hundreds of kilometers for a large river (e.g., a 30 m deep river with 50 m²/s width-averaged water discharge on a 5×10^{-5} slope).

The sediment flux delivered to the coasts in RAFEM is reworked by the wave-driven alongshore sediment transport in CEM (A. Ashton et al., 2001; A. D. Ashton & Murray, 2006a, 2006b). The erosion or accretion of the coastline occurs where there is a gradient in net alongshore sediment transport. Assuming conservation of near-shore sand and a long-term constant shoreface profile, shoreline change is calculated by:

$$\frac{d\eta}{dt} = -\frac{1}{D_{sf}} \frac{dQ_s}{dx} \tag{1}$$

where η is cross-shore shoreline position, t is time, Q_s is the volumetric wave-driven alongshore sediment transport, D_{st} is the shoreface depth, x is the alongshore direction.

In CEM, wave height is held constant during each experiment, representing effective average wave height (A. D. Ashton & Murray, 2006a). Wave climate is defined by the fraction of offshore high angles waves (U) and the fraction of waves approaching from the left relative to the initial, overall coastline orientation (wave asymmetry, A) and is presented in the form of probability density function (wave climate PDF, see Figure 8 of A. D. Ashton & Murray, 2006a). Offshore wave approach angles are randomly selected from the wave climate PDF and change every simulated day. Within the wave climate PDF, the probability of each angle bin represents the cumulative influence from waves within that range of directions (A. D. Ashton & Murray, 2006b). U and wave height affect wave-climate diffusivity. Smaller U value suggests greater influence from low-angle waves, which tend to smooth the coastline. U > 0.5 indicates a net anti-diffusive wave climate, which causes coastline perturbations to grow. In our experiments, we used U parameters varying between 0.3 and 0.5 to model diffusive wave climates. When A = 0.5, the shoreline experiences a symmetric mix of influences from both sides of the delta. In asymmetric wave climate experiments with A > 0.5, the shoreline experiences stronger influences of waves approaching the coastline from the left (looking offshore), resulting in net alongshore sediment transport from left to right. We tested A values between 0.6 and 0.9 in model experiments to explore the dependence of delta morphology and avulsion dynamics to varying wave-climate asymmetry.

2.2. Data Analysis

Every approaching wave can cause some alongshore sediment transport and coastline shape change. The shoreline diffusivity associated with each wave-approach direction depends on the difference between the angle of offshore wave crests (\emptyset_0) and the angle of the shoreline (θ):

$$\mu = -\frac{K_2}{D_{sf}} T^{1/5} H_0^{12/5} \left\{ \cos^{1/5} (\emptyset_0 - \theta) \left[\left(\frac{6}{5} \right) \sin^2 (\emptyset_0 - \theta) - \cos^2 (\emptyset_0 - \theta) \right] \right\}$$
 (2)

HU ET AL. 3 of 10



where K_2 is ~0.34 m^{3/5}s^{-6/5} (A. D. Ashton & Murray, 2006b), T is wave period, and H_0 is the offshore wave height. ("Offshore" here refers to the offshore limit of approximately shore-parallel depth contours, i.e., the base of the shoreface.) The long-term effective shoreline diffusivity is the summed diffusivities for waves from all angle bins, weighted by the probabilities in each bin (using one-degree increments). The global, overall shoreline angle is used for calculating regional diffusivity, while the local shoreline angle (a four-cell moving average) is used for calculating the local effective diffusivity.

To constrain the statistical uncertainties, we used three groups of random elevation perturbations added to the initial downstream-sloping landscape. In each group of experiments, we compared local shoreline angles to identify the maximum magnitude of the shoreline angle relative to the overall coastline orientation for both updrift and downdrift flanks. Then, we measured the delta morphological responses to wave-climate asymmetry through the degree of delta asymmetry, A_{delta} , defined by the ratio of the maximum magnitude of the shoreline angle updrift and downdrift of the tip of the delta:

$$A_{delta} = |\theta_{maxu}|/|\theta_{maxd}| \tag{3}$$

The tip of the delta is defined as the shoreline cell that extends farthest seaward (in the global cross-shore direction). The degree of delta asymmetry is calculated at every $\sim 31T_{cf}$ over a modeled time of $\sim 12600T_{cf}$ and averaged for each wave climate experiment. When $A_{delta}=1$, the delta morphology is symmetric. The more A_{delta} deviates from 1, the greater the delta morphological asymmetry is. When the river avulses to updrift of the delta tip, we consider the avulsion an updrift avulsion. To capture the tendency toward updrift avulsions under various wave climate scenarios, we calculated the fraction of time that the river avulses to the updrift delta flank.

3. Results and Discussion

3.1. Delta Morphologies

The couplings between shoreline and river dynamics in this model framework lead to a dependence of delta plan view morphology on wave climate diffusivity (determined by WH and U; Figure 1; Ratliff et al., 2018), and on wave climate asymmetry (Figure 1). To quantify the relative influence of the river and waves on delta morphology, we used the ratio of the fluvial sediment flux leaving the river mouth to the maximum possible alongshore transport away from the river mouth, for a given wave climate, R (Nienhuis et al., 2015). In our model experiments, deltas are river-dominated (R > 1) with small wave height (WH = 0.3). With larger wave height (WH = 0.4), deltas are strongly wave influenced (R < 1) when diffusive waves dominate the wave climate, while deltas become river-dominated (R > 1) when wave climate diffusivity decreases (Figure S1 in Supporting Information S1). When R > 1, wave influences become neglectable and therefore the effect of wave asymmetry becomes less important. To investigate how wave climate asymmetry strongly affects wave-influenced deltas, we concentrated our analyses on experiments using WH = 0.5, which have R < 1 for all values of U used in this study (Figure 1). Experiments using WH = 0.4 showed the same trends in morphology (Figure S1 in Supporting Information S1).

In our model experiments, the input wave climate is defined relative to the regional, overall coastline orientation. In this case, diffusivity varies with offshore wave angle, from a maximum when the wave approaches directly onshore (shore-normal) to 0 when the wave angle is ~45° (see Figure 4 of A. D. Ashton & Murray, 2006a). However, the wave-climate diffusivity felt by shorelines locally can vary considerably from the regionally defined wave climate (A. D. Ashton & Murray, 2006b), because (a) changing the local shoreline angle changes wave angles relative to the local shoreline, and (b) some of the waves in the regional climate do not reach all local shorelines.

When the wave climate is asymmetric, waves approach the shoreline dominantly from one direction (the left in our experiments). Local shorelines on the updrift flank are rotated toward the dominant wave direction. Most waves from the dominant direction approach the rotated local shorelines on the updrift flank from lower angles, relative to the regional shoreline orientation, increasing their diffusional effects locally. Thus, for the rotated shoreline on the updrift flank, effective diffusivity is higher. In contrast, shorelines on the downdrift flank are rotated such that waves from dominant direction approach local shorelines from a higher angle, decreasing the effective diffusivity locally (Figure 1).

HU ET AL. 4 of 10



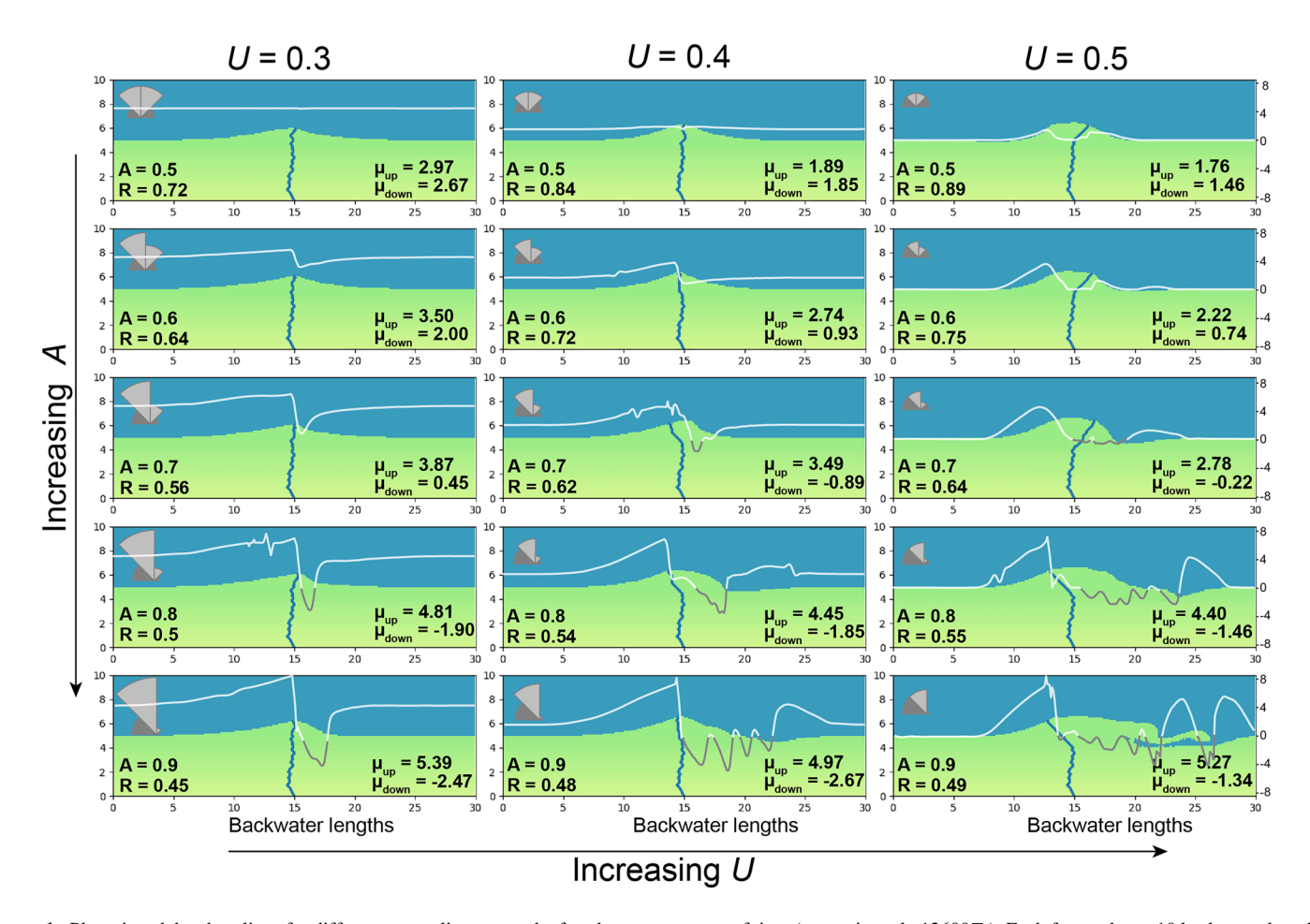


Figure 1. Plan-view delta shorelines for different wave climates, each after the same amount of time (approximately $12600T_{cf}$). Each frame shows 10 backwater lengths in the cross-shore direction and 30 backwater lengths alongshore. In all simulations, wave height (0.5), sea-level rise rate (0.0), and critical SER (1.0) are held constant. High angle wave fraction (i.e., wave diffusivity for the overall coastline orientation) increases from left to right, reducing the overall shoreline diffusivity. Wave climate asymmetry increases from top to bottom. Overlaid lines show the local diffusivity along the shoreline, with positive diffusivity in white, and negative in gray (scale on the right side of panels). μ_{up} is the effective diffusivity where the local shoreline angle deviates most from the regional angle on the updrift flank, and μ_{down} is the effective diffusivity where the local shoreline angle deviates most on the downdrift flank.

The discrepancy in effective diffusivities between the updrift and downdrift flank leads to different shoreline curvatures. As both flanks prograde at approximately the same rate, a lower curvature develops on the updrift flank, while a greater curvature develops on the downdrift flank, as long as local effective diffusivity remains positive there (Figures 1 and 2c). If the downdrift effective diffusivity approaches zero or becomes negative, convex curvature can persist and even be associated with progradation (for negative diffusivity; Figures 1 and 2g).

As *U* increases, and regional effective diffusivity comes closer to 0, less downdrift shoreline rotation is required for local effective diffusivity to become negative, and the downdrift shoreline has a greater chance to develop convex curvature. Under these conditions, as the downdrift flank progrades, it can block part of the shoreline from waves from the dominant direction and create a "wave-shadowed zone" downdrift. Long-term net sediment transport is reduced within the wave-shadowed zone, and an associated sediment flux gradient causes erosion downdrift of location of maximum shadowing (A. D. Ashton & Murray, 2006a; evident in Figure 1, lower right panels).

3.2. River Avulsion Dynamics

As the river attains sufficient superelevation to avulse at some point (i.e., the "avulsion node"), possible locations for the new post-avulsion river mouth are constrained by shoreline shape (which evolves between avulsions in response to waves and sediment delivery at the present river mouth location), because the path from the avulsion

HU ET AL. 5 of 10

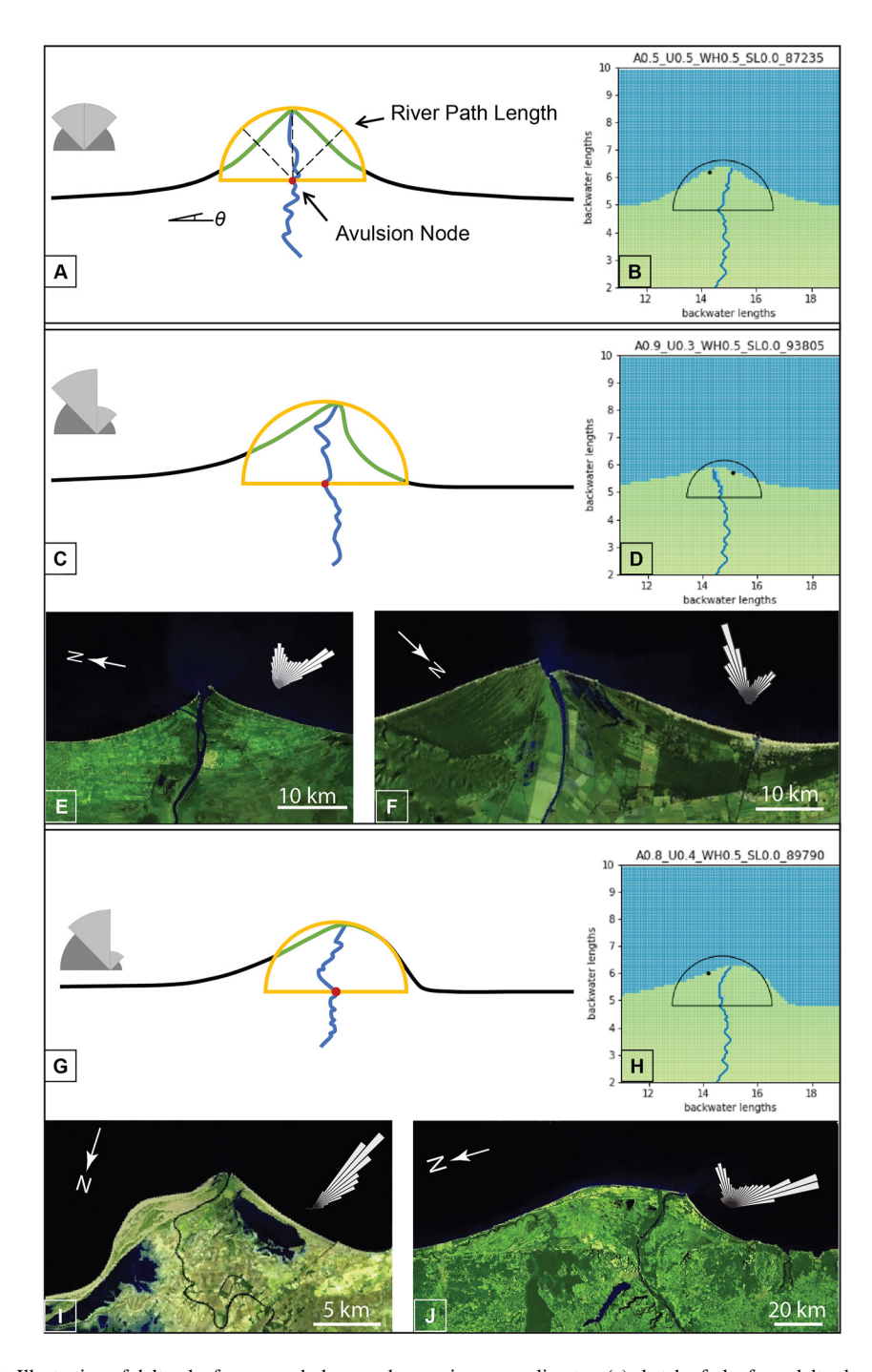


Figure 2. Illustration of delta planform morphology under varying wave climates: (a) sketch of planform delta shorelines under a symmetric wave climate, with the semi-circle (yellow) that outlines possible river avulsion locations (green lines) and the river avulsion node (red dot); (b) river can avulse to either side of a concave shoreline with symmetric wave climates, (c) sketch of planform delta shorelines under asymmetric and diffusive wave climates; (d) low updrift shoreline concavity limits the possibility of updrift river avulsion; (e) Rio Grijalva, Mexico; (f) Ombrone river, Italy; (g) sketch of planform delta shorelines under very asymmetric or less diffusive wave climates; (h) downdrift convexity favors updrift river avulsion; (i) Ceyhan river, Turkey; (e) Doce river, Brazil. Remote sensing images are from Sentinel-2. Wave-Watch data are from National Oceanic and Atmospheric Administration (NOAA) and is organized by Nienhuis et al. (2020).

node to the new river mouth location must be shorter than the present path for an avulsion to occur in the model. This constraint can be illustrated by a semi-circle, centered on the avulsion node, with a radius equal to the average of the current river path length (including sinusity) and the straight-line distance from the avulsion node to

HU ET AL. 6 of 10



the present river mouth (Figure 2). For river courses with negligible sinuosity, the river can only avulse to shoreline locations that fall on the landward side of the semicircle. Assuming a landscape topography that is equally likely to steer a new steepest descent path to either side, the probability of an updrift avulsion is proportional to the ratio between the lengths of the shoreline the river can avulse to updrift and downdrift.

With a symmetric or slightly asymmetric (and diffusive) wave climate, the shorelines on both flanks of the delta will be concave seaward, so that the river can avulse to both sides of the delta near the delta tip (Figure 2a). Asymmetric wave climates impose two opposing restrictions on possible avulsion locations.

3.2.1. Updrift and Downdrift Concave Curvatures

The low curvature on the updrift delta flank, resulting from the high effective diffusivity of the local wave climate, tends to restrict the updrift locations the river can avulse to. Conversely, the lower effective diffusivity on the downdrift flank tends to cause larger shoreline curvature, expanding the length of shoreline viable for avulsion (Figure 2c). As the downdrift shoreline becomes more accessible, the river tends to avulse to the downdrift side of the delta tip (Figure 2d). In cases where these curvature effects lead to a predominance of downdrift avulsions, some of the avulsions still move the river mouth back in the updrift direction. This occurs because once the river avulses to a downdrift location, the fluvial sediment input tends to promote shoreline progradation there (Movie S1).

3.2.2. Downdrift Convexity

With decreasing diffusivity of the regional wave climate (i.e., greater U values) and increasing wave asymmetry, the local diffusivity on the downdrift flank approaches zero. When diffusivity becomes sufficiently small, the shoreline will no longer maintain the concave shape; sediments transported downdrift from the river mouth cannot be distributed along the downdrift shoreline rapidly enough, and the downdrift flank becomes convex (Figure 2g). If the local downdrift diffusivity becomes negative, the convexity will enhance progradation. As a result, the delta tends to migrate in the downdrift direction, extending the distance between the avulsion node and shorelines on the downdrift flank. In addition, with if the delta migrates alongshore, the updrift shoreline will experience erosion, bringing the updrift shoreline closer to the avulsion node. Both progradation on the downdrift flank and erosion on the updrift flank tend to make the updrift side of the delta becomes the preferred avulsion location (Figures 2g and 2h). With increasingly asymmetric wave climates, downdrift delta migration is more rapid. Although the downdrift delta movement limits downdrift avulsion in most cases, continuous fluvial input can develop a new delta tip on the updrift side of the initial avulsion node. With stronger wave diffusivity on the updrift flank, downdrift avulsion relative to the newly developed delta tip is still possible (Movie S2).

3.3. Dominant Effects Vary With Wave Climate

To characterize river avulsion tendencies under various wave climates, we calculated the fraction of avulsions that move the river mouth to the updrift side of the delta tip (Figure 3a). When the diffusivity of the regional wave climate is high enough to distribute fluvial sediment widely along the shoreline, the delta progrades slowly, and the progradation-related aggradation of the river profile is also inhibited (Ratliff et al., 2018). During the model experiments (each lasting for $\sim 12600T_{cf}$), fewer avulsions occur as regional wave climate diffusivity increases (U decreases).

With slight wave asymmetry (A = 0.6), delta morphology is only slightly asymmetric (Figures 1 and 3b), and avulsions occur approximately as often to the downdrift and updrift sides of the delta tip (Figure 3a). With high regional wave climate diffusivity (low U in model experiments), as the wave climate becomes more asymmetric, the effect of decreased updrift curvature becomes more dominant, and downdrift avulsions become more frequent (Figure 3a). The increases in wave climate asymmetry impose greater delta plan-form asymmetry (Figure 3b; Figure S3 in Supporting Information S1).

With lower regional wave climate diffusivity (higher U), increasing wave-climate asymmetry favors the downdrift-convexity effect, leading to a more asymmetric delta plan-form morphology (Figure 3b; Figure S3 in Supporting Information S1). The tendency for reduced updrift concavity competes with the tendency for downdrift convexity in determining the updrift/downdrift avulsion tendency. With a wave-climate asymmetry of 0.7 and 0.8, reduced updrift concavity controls the avulsion tendency in the early stage of the delta evolution. However, as the delta cross-shore/alongshore aspect ratio becomes more pronounced and the diffusivity on the

HU ET AL. 7 of 10



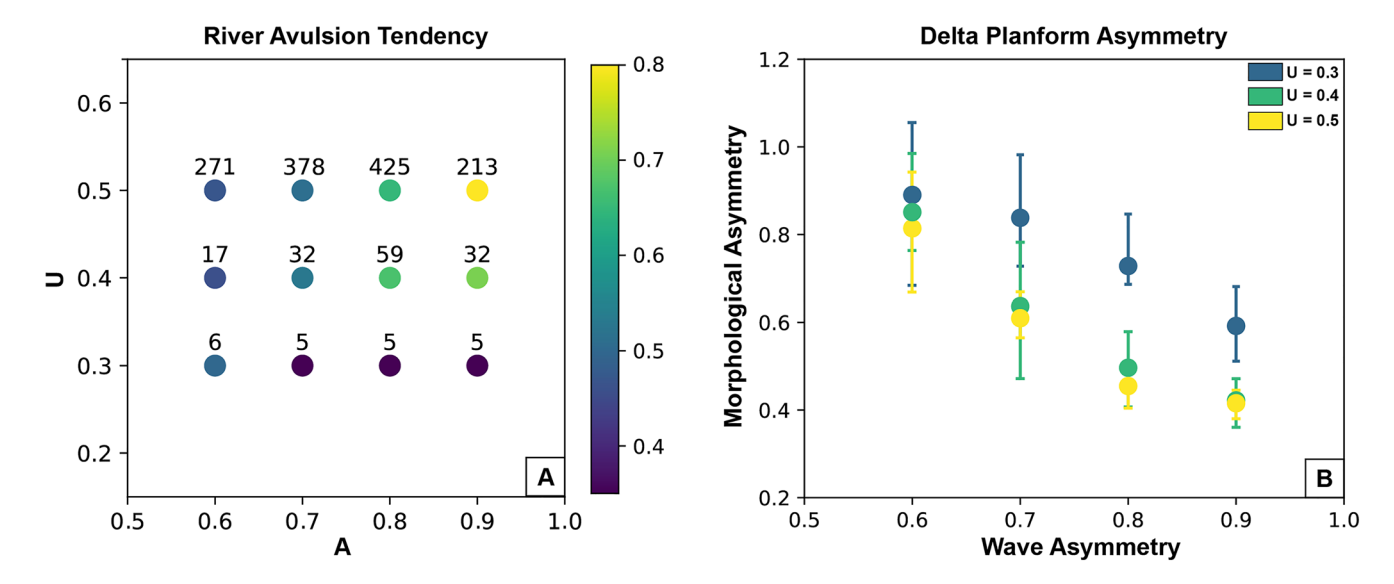


Figure 3. Comparison of river avulsion tendency and delta planform asymmetry under various wave climates. (a) River avulsion tendency. Color shows the percent of avulsions to the updrift side of the delta tip. The number of avulsions (summed over three replicates) is shown above each dot. (b) Delta planform asymmetry. Delta morphology is symmetric when the $A_{delta} = 1$.

downdrift shoreline decreases, the effects of downdrift convexity lead to a predominance of updrift avulsions (Movie S1). When the wave climate is extremely asymmetric (A = 0.9), the downdrift convexity effect dominates more consistently, leading to a preponderance of updrift avulsions (Figure 3a). On the other hand, reduced updrift concavity can also limit the updrift shoreline accessibility, restricting the possible avulsion locations. As a result, the river mouth location varies little when the regional wave diffusivity is small, and the river mouth location after avulsions tend to be on the updrift flank. Restricting the potential paths for successful avulsions manifests as a higher percent of failed avulsions during model experiments (Table S2 in Supporting Information S1).

3.4. Critical Superelevation Ratio Effects

The updrift/downdrift river avulsion tendency and delta morphology are also influenced by the critical SER (Figure S4 in Supporting Information S1). Decreasing the critical SER value reduces the amount of channel aggradation required to trigger an avulsion, so the avulsion time scale decreases. More frequent shifts in river mouth location augment the effects of a diffusive wave climate, tending to produce a smoother shoreline. Because the delta cross-shore/alongshore aspect ratio is reduced with a lower critical SER, shoreline orientations on the updrift and downdrift flanks of the delta deviate less from the regional coastline orientation (relative to the case with a higher critical SER). With smaller decreases in diffusivity on the downdrift flanks, the tendency for downdrift convexity, and consequently updrift avulsions, is reduced (Figure S4 in Supporting Information S1).

4. Implications and Future Work

Future work will be needed to systematically compare model results to natural deltas. The quantitative analysis of wave climates for natural deltas (e.g., A. D. Ashton & Murray, 2006b) is beyond the scope of this work. However, in the initial comparisons shown here, wave-influenced deltas exhibit the asymmetry of shoreline curvature we would expect from the variation of local effective shoreline diffusivity, based on model results (Figure 1). As wave-climate asymmetry tends to locally increase the shoreline smoothing effect of gradients in net alongshore sediment transport on the updrift delta flank, updrift delta flanks tend to be straighter than the downdrift flank (Figures 2e and 2f). When the wave-climate asymmetry becomes extreme, local effective diffusivity on the downdrift flank can become sufficiently small, leading to convex downdrift shorelines (Figures 2i and 2j). In the case of the Doce river shown in Figure 2j, the convexity on the downdrift flank corresponds to a former river mouth location. However, the fact that the convexity still exits ~5,000 years after the river avulsed to the present location (Rossetti et al., 2015) is consistent with a very small or negative local diffusivity.

HU ET AL. 8 of 10



Acknowledgments

(1831623).

We thank for Katherine Anarde and

Jaap Nienhuis for insightful discussions

about this work. We thank Maarten van

for helpful comments. We acknowledge

High-Performance Computing Cluster.

CSDMS gratefully acknowledges major

funding through a cooperative agreement

with the National Science Foundation

der Vegt and an anonymous reviewer

computing time on the CU-CSDMS

Since most natural shorelines are exposed to asymmetric wave climates, as deltas become more wave-dominated, not only will avulsions tend to occur less frequently (Ratliff et al., 2018), the tendency for updrift or downdrift avulsions will also play a more important role in understanding and forecasting delta evolution in natural settings. Ultimately, understanding the processes that influence where new river courses and river mouths tend to be located could help inform decision making in coastal zones.

Additionally, we found that although the effective diffusivity for the global average coastline orientation is independent of wave-climate asymmetry, the maximum potential local effective diffusivity, which could be realized for a particular local shoreline orientation, increases with wave-climate diffusivity (Text S3 in Supporting Information S1), which have broader implications for coastline evolution beyond the scope of deltas.

The coupled model excludes some processes that may affect river avulsion dynamics. For example, in our model, when the delta is strongly influenced by an asymmetric wave climate (high A, small U/Large WH), river avulsion frequency tends to be reduced because waves can effectively redistribute sediments, which slows down the in-channel aggradation rate. The river-mouth dynamics model by Gao et al. (2020) has shown that, under similar circumstances, the large net alongshore sediment transport can enhance the progradation of a downdrift-deflected channel if sediment bypassing of the river mouth is limited. This effect, which would tend to increase avulsion frequency, is not accounted for here. Future work including the river-mouth processes in this coupled modeling framework could enhance the understanding of how river processes respond to diffusive and asymmetric wave climates. However, the results we emphasize here, involving how subsequent river mouth locations are influenced by delta shape as it responds to the wave-climate, are unlikely to be qualitatively affected by the addition of river-mouth-migration dynamics. The effect of changing sea-level on river processes and delta morphology under asymmetric wave climates requires additional research. In addition, because shorelines on the updrift and downdrift flanks show different responses to the asymmetric wave climate, deltas under asymmetric wave climates may form characteristic stratigraphy over time, which could be useful for stratigraphic interpretation in deltaic environments.

Data Availability Statement

RAFEM and CEM are available through the model repository on the CSDMS website (https://csdms.colorado.edu/wiki/Model:RAFEM and https://csdms.colorado.edu/wiki/Model:CEM). The coupled model is currently available on Zenodo (https://zenodo.org/badge/latestdoi/458204057).

References

Ashton, A., Murray, A. B., & Arnoult, O. (2001). Formation of coastline features by large-scale instabilities induced by high-angle waves. *Nature*, 414(6861), 296–300. https://doi.org/10.1038/35104541

Ashton, A. D., & Giosan, L. (2011). Wave-angle control of delta evolution. Geophysical Research Letters, 38(13). https://doi.org/10.1029/2011gl047630

Ashton, A. D., Hutton, E. W., Kettner, A. J., Xing, F., Kallumadikal, J., Nienhuis, J., & Giosan, L. (2013). Progress in coupling models of coastline and fluvial dynamics. *Computers & Geosciences*, 53, 21–29. https://doi.org/10.1016/j.cageo.2012.04.004

Ashton, A. D., & Murray, A. B. (2006a). High-angle wave instability and emergent shoreline shapes: 1. Modeling of sand waves, flying spits, and capes. *Journal of Geophysical Research*, 111(F4), F04011. https://doi.org/10.1029/2005JF000422

Ashton, A. D., & Murray, A. B. (2006b). High-angle wave instability and emergent shoreline shapes: 2. Wave climate analysis and comparisons to nature. *Journal of Geophysical Research*, 111(F4), F04012. https://doi.org/10.1029/2005JF000423

Chadwick, A. J., Lamb, M. P., Moodie, A. J., Parker, G., & Nittrouer, J. A. (2019). Origin of a preferential avulsion node on lowland river deltas. Geophysical Research Letters, 46, 4267–4277. https://doi.org/10.1029/2019GL082491

Chatanantavet, P., Lamb, M. P., & Nittrouer, J. A. (2012). Backwater controls of avulsion location on deltas. *Geophysical Research Letters*, 39(1), L01402. https://doi.org/10.1029/2011GL050197

Dean, R., & Yoo, C. H. (1992). Beach-nourishment performance predictions. *Journal of Waterway, Port, Coastal, and Ocean Engineering*, 118(6), 567–586. https://doi.org/10.1061/(ASCE)0733-950X(1992)118:6(567)

Falqués, A., & Calvete, D. (2005). Large-scale dynamics of sandy coastlines: Diffusivity and instability. *Journal of Geophysical Research*, 110, C03007. https://doi.org/10.1029/2004JC002587

Galloway, W. E. (1975). Process framework for describing the morphologic and stratigraphic evolution of deltaic depositional systems.

Ganti, V., Chadwick, A. J., Hassenruck-Gudipati, H. J., Fuller, B. M., & Lamb, M. P. (2016). Experimental river delta size set by multiple floods and backwater hydrodynam-ics. *Science Advances*, 2(5), e1501768. https://doi.org/10.1126/sciadv.1501768

Gao, W., Nienhuis, J., Nardin, W., Wang, Z. B., Shao, D., Sun, T., & Cui, B. (2020). Wave controls on deltaic shoreline-channel morphodynamics: Insights from a coupled model. *Water Resources Research*, 56(9), e2020WR027298. https://doi.org/10.1029/2020WR027298

Hajek, E. A., & Wolinsky, M. A. (2012). Simplified process modeling of river avulsion and alluvial architecture: Connecting models and field data. Sedimentary Geology, 257, 1–30. https://doi.org/10.1016/j.sedgeo.2011.09.005

Jerolmack, D. J. (2009). Conceptual framework for assessing the response of delta channel networks to Holocene sea level rise. Quaternary Science Reviews, 28(17–18), 1786–1800.

HU ET AL. 9 of 10



- Jerolmack, D. J., & Paola, C. (2007). Complexity in a cellular model of river avulsion. Geomorphology, 91(3), 259–270. https://doi.org/10.1016/j.geomorph.2007.04.022
- Komar, P. D. (1973). Computer models of delta growth due to sediment input from rivers and longshore transport. The Geological Society of America Bulletin, 84(7), 2217–2226. https://doi.org/10.1130/0016-7606(1973)84<2217:cmodgd>2.0.co;2
- Lauzon, R., Murray, A. B., Cheng, S., Liu, J., Ells, K. D., & Lazarus, E. D. (2019). Correlation between shoreline change and planform curvature on wave-dominated, sandy coasts. *Journal of Geophysical Research: Earth Surface*, 124(12), 3090–3106. https://doi.org/10.1029/2019jf005043
- Mohrig, D., Heller, P. L., Paola, C., & Lyons, W. J. (2000). Interpreting avulsion process from ancient alluvial sequences: Guadalope-Matarranya system (northern Spain) and Wasatch Formation (Western Colorado). *The Geological Society of America Bulletin*, 112(12), 1787–1803. https://doi.org/10.1130/0016-7606(2000)112<1787:iapfaa>2.0.co;2
- Nienhuis, J. H., Ashton, A. D., Edmonds, D. A., Hoitink, A. J. F., Kettner, A. J., Rowland, J. C., & Törnqvist, T. E. (2020). Global-scale human impact on delta morphology has led to net land area gain. *Nature*, 577(7791), 514–518. https://doi.org/10.1038/s41586-019-1905-9
- Nienhuis, J. H., Ashton, A. D., & Giosan, L. (2015). What makes a delta wave-dominated? *Geology*, 43(6), 511–514. https://doi.org/10.1130/G36518.1
- Nienhuis, J. H., Ashton, A. D., Nardin, W., Fagherazzi, S., & Giosan, L. (2016). Alongshore sediment bypassing as a control on river mouth morphodynamics. *Journal of Geophysical Research: Earth Surface*, 121(4), 664–683. https://doi.org/10.1002/2015jf003780
- Nienhuis, J. H., Rnqvist, T. E., & Esposito, C. R. (2018). Crevasse splays versus avulsions: A recipe for land building with levee breaches (Vol. 45, pp. 4058–4067). https://doi.org/10.1029/2018GL077933
- Orton, G. J., & Reading, H. G. (1993). Variability of deltaic processes in terms of sediment supply, with particular emphasis on grain size. Sedimentology, 40(3), 475–512. https://doi.org/10.1111/j.1365-3091.1993.tb01347.x
- Paola, C. (2000). Quantitative models of sedimentary basin filling. Sedimentology, 47(s1), 121–178. https://doi.org/10.1046/j.1365-3091.2000.00006.x
- Peckham, S. D., Hutton, E. W., & Norris, B. (2013). A component-based approach to integrated modeling in the geosciences: The design of CSDMS. *Computers & Geosciences*, 53, 3–12. https://doi.org/10.1016/j.cageo.2012.04.002
- Pittaluga, M., Repetto, R., & Tubino, M. (2003). Channel bifurcation in braided rivers: Equilibrium configurations and stability. Water Resources Research, 39(3). https://doi.org/10.1029/2001wr001112
- Ratliff, K. M., Hutton, E. H., & Murray, A. B. (2018). Exploring wave and sea-level rise effects on delta morphodynamics with a coupled river-ocean model. *Journal of Geophysical Research: Earth Surface*, 123(11), 2887–2900. https://doi.org/10.1029/2018jf004757
- Rossetti, D. d. F., Polizel, S. P., Cohen, M. C. L., & Pessenda, L. C. R. (2015). Late Pleistocene Holocene evolution of the Doce River delta, southeastern Brazil: Implications for the understanding of wave-influenced deltas. *Marine Geology*, 367, 171–190. https://doi.org/10.1016/j.margeo.2015.05.012
- Slingerland, R., & Smith, N. D. (2004). River avulsions and their deposits. Annual Review of Earth and Planetary Sciences, 32, 257–285. https://doi.org/10.1146/annurev.earth.32.101802.120201
- Syvitski, J. P., Kettner, A. J., Overeem, I., Hutton, E. W., Hannon, M. T., Brakenridge, G. R., et al. (2009). Sinking deltas due to human activities. Nature Geoscience, 2(10), 681–686. https://doi.org/10.1038/ngeo629
- Wright, L. D., & Coleman, J. M. (1973). Variations in morphology of major river deltas as functions of ocean wave and river discharge regimes. AAPG Bulletin, 57(2), 370–398.

References From the Supporting Information

- Chadwick, A. J., & Lamb, M. P. (2021). Climate-change controls on river delta avulsion location and frequency. *Journal of Geophysical Research:* Earth Surface, 126(6), e2020JF005950. https://doi.org/10.1029/2020jf005950
- Hutton, E. W., & Syvitski, J. P. (2008). Sedflux 2.0: An advanced process-response model that generates three-dimensional stratigraphy. Computers & Geosciences, 34(10), 1319–1337. Predictive Modeling in Sediment Transport and Stratigraphy. https://doi.org/10.1016/j.cageo.2008.02.013
 Jerolmack, D. J., & Paola, C. (2007). Complexity in a cellular model of river avulsion. Geomorphology, 91(3), 259–270. https://doi.org/10.1016/j.geomorph.2007.04.022
- Ratliff, K. M., Hutton, E. W., & Murray, A. B. (2021). Modeling long-term delta dynamics reveals persistent geometric river avulsion locations. Earth and Planetary Science Letters, 559, 116786. https://doi.org/10.1016/j.epsl.2021.116786

HU ET AL. 10 of 10